Aquaporins facilitate hydrogen peroxide entry into guard cells to mediate ABA- and pathogen-triggered stomatal closure.

Olivier Rodrigues, Ganna Reshetnyak, Alexandre Grondin, Yusuke Saijo, Nathalie Leonhardt, Christophe Maurel, Lionel Verdoucq

Aquaporins facilitate hydrogen peroxide entry into guard cells to mediate ABA- and pathogen-triggered stomatal closure

Olivier Rodrigues[a], Ganna Reshetnyak[a], Alexandre Grondin[a,1], Yusuke Saijo[b], Nathalie Leonhardt[c], Christophe Maurel[a], and Lionel Verdoucq[a,2]

[a]Biochimie et Physiologie Moléculaire des Plantes, Unité Mixte de Recherche 5004, CNRS/Institut National de la Recherche Agronomique/Montpellier SupAgro/Université de Montpellier, F-34060 Montpellier Cedex 2, France; [b]Department of Biology, Nara Institute of Science and Technology, Ikoma, 630-0192, Japan; and [c]Laboratoire de Biologie du Développement des Plantes, French Alternative Energies and Atomic Energy Commission (CEA) Cadarache, Unité Mixte de Recherche 7265, CNRS/CEA/Aix-Marseille Université, F-13108 Saint-Paul-lez-Durance, France

Edited by Maarten J. Chrispeels, University of California, San Diego, La Jolla, CA, and approved July 14, 2017 (received for review March 27, 2017)

Stomatal movements are crucial for the control of plant water status and protection against pathogens. Assays on epidermal peels revealed that, similar to abscisic acid (ABA), pathogen-associated molecular pattern (PAMP) flg22 requires the *At*PIP2;1 aquaporin to induce stomatal closure. Flg22 also induced an increase in osmotic water permeability (P_f) of guard cell protoplasts through activation of *At*PIP2;1. The use of HyPer, a genetic probe for intracellular hydrogen peroxide (H_2O_2), revealed that both ABA and flg22 triggered an accumulation of H_2O_2 in wild-type but not *pip2;1* guard cells. Pretreatment of guard cells with flg22 or ABA facilitated the influx of exogenous H_2O_2. Brassinosteroid insensitive 1-associated receptor kinase 1 (BAK1) and open stomata 1 (OST1)/Snf1-related protein kinase 2.6 (SnRK2.6) were both necessary to flg22-induced P_f and both phosphorylated *At*PIP2;1 on Ser121 in vitro. Accumulation of H_2O_2 and stomatal closure as induced by flg22 was restored in *pip2;1* guard cells by a phosphomimetic form (Ser121Asp) but not by a phosphodeficient form (Ser121Ala) of *At*PIP2;1. We propose a mechanism whereby phosphorylation of *At*PIP2;1 Ser121 by BAK1 and/or OST1 is triggered in response to flg22 to activate its water and H_2O_2 transport activities. This work establishes a signaling role of plasma membrane aquaporins in guard cells and potentially in other cellular context involving H_2O_2 signaling.

aquaporin | pathogen | guard cell signaling | hydrogen peroxide | stomatal movement

Stomata are specialized pores formed by two guard cells at the surface of plant aerial parts. Stomata mediate gas exchange between the plant and atmosphere, thereby acting on both the rate of photosynthesis and plant water status (1). Their opening and closing, as triggered by numerous endogenous and environmental stimuli, involve combined movements of ions and water across the guard cell plasma membrane, which, in turn, alter guard cell turgor and volume (2). Abscisic acid (ABA), a key hormone in plant response to water deficit, is a potent inducer of stomatal closure (3). ABA binds to PYR/PYL/RCAR receptors, which capture protein phosphatases 2C (4), leading to activation of Snf1-related protein kinases 2 such as SnRK2.6/OST1 (5). This protein kinase, in turn, activates several types of membrane proteins involved in stomatal closure such as NADPH oxidases (6, 7); the anion channels SLAC1, SLAH1, and SLAH3 (8–10); and the plasma membrane aquaporin (AQP) *At*PIP2;1 (11).

Stomata are also a potential entry gate for pathogens. While plants have the capacity to close their stomata after perception of pathogen-associated molecular patterns (PAMPs) or damaged associated molecular patterns (DAMPs) (12), some pathogens can, in turn, thwart the stomatal closure by means of effectors such as coronatine (12) or HoPM1 (13). Signaling pathways involved in guard cell response to pathogens have been the focus of recent studies (14). Notably, flg22 (a PAMP from the bacterium *Pseudomonas syringae* pv. *tomato*) is perceived by the receptor kinase FLS2 which, in interaction with BAK1 and BIK1 protein kinases (15), activates NADPH oxidases (16). In conjunction with superoxide dismutases (SOD) and cell wall peroxidases (17), the latter triggers apoplastic production of reactive oxygen species (ROS) (18) and, as a consequence, marked accumulation of hydrogen peroxide (H_2O_2) in the guard cell cytoplasm. Alternative signaling mechanisms acting downstream of flg22 perception have been proposed. Flg22 would target the same SLAC1 anion channel as ABA does, but through an oxylipin-dependent ABA-independent pathway (19) that merges at OST1 (20).

A role for AQPs was recently established in *Arabidopsis thaliana* guard cells (11). Plants lacking *At*PIP2;1 showed defects in ABA-triggered stomatal closure in epidermal peel assays. This phenotype was associated to cellular defects in both plasma membrane water transport and hormone signaling (ROS accumulation). Furthermore, ABA was found to activate *At*PIP2;1 through OST1-mediated phosphorylation of a key cytoplasmic residue (Ser121), this modification being mandatory for ABA-induced stomatal closure (11).

Recent studies have revealed that the function of plant AQPs extends beyond water transport (21). For instance, members of the plasma membrane intrinsic protein (PIP) subfamily facilitate carbon dioxide (CO_2) (22) or H_2O_2 (23, 24) transport in

Significance

Guard cells play a crucial role in controlling transpiration and the plant water status. Here, we show that the *Arabidopsis* plasma membrane aquaporin PIP2;1 is involved in stomatal closure triggered by abscisic acid (ABA) or the pathogen-associated molecular pattern flg22. The use of a genetic probe for hydrogen peroxide (H_2O_2) revealed that PIP2;1 is also required for intracellular accumulation of H_2O_2 after flg22 or ABA treatments. Our data lead to a model whereby flg22 and ABA activate PIP2;1 through phosphorylation at a conserved site to facilitate transport of both water and H_2O_2 and promote stomatal closure. This study fills a gap in our understanding of stomatal regulation and suggests a general signaling role of aquaporin in contexts involving H_2O_2.

Author contributions: O.R., C.M., and L.V. designed research; O.R., G.R., and L.V. performed research; O.R., A.G., Y.S., N.L., and L.V. contributed new reagents/analytic tools; O.R., G.R., and L.V. analyzed data; and O.R., C.M., and L.V. wrote the paper.

The authors declare no conflict of interest.

This article is a PNAS Direct Submission.

[1]Present address: UMR Plant Diversity Adaptation and Development - Research Unit (DIADE), Institut de Recherche pour le Développement/Université de Montpellier, F-34394 Montpellier Cedex 5, France.

[2]To whom correspondence should be addressed. Email: lionel.verdoucq@cnrs.fr.

This article contains supporting information online at www.pnas.org/lookup/suppl/doi:10.1073/pnas.1704754114/-/DCSupplemental.

heterologous systems. A contribution of *At*PIP2;1 to guard cell CO_2 transport was recently proposed, based on functional reconstitution of CO_2 signaling in *Xenopus* oocytes (25). The significance of H_2O_2 transport by plant AQPs with respect to ROS metabolism and detoxification or ROS-dependent signaling in guard cells has not yet been elucidated. By contrast, a role for *At*PIP1;4-mediated H_2O_2 transport in plant immunity against the bacterial pathogen *Pseudomonas synringae* was recently uncovered (26).

In the present work, we used the context of stimulus-induced guard cell movements to explore a putative role of AQPs in plant cell signaling. A key point was to express the genetically encoded fluorescent H_2O_2 sensor, HyPer (27), in plant lines altered in *At*PIP2;1 function and regulation. Our data establish the significance of H_2O_2 transport by plant AQPs during both ABA- and flg22-induced stomatal closure and uncover common signaling components acting on AQP activity.

Results

HyPer Allows Monitoring of H_2O_2 Abundance in Guard Cells. The expression and subcellular localization of HyPer in guard cells was followed by fluorescence microscopy on isolated leaf epidermis. HyPer fluorescence was essentially observed (Fig. S1*A*) in the nucleus, perinuclear areas, and close to the plasma membrane, in regions where the cytoplasm is reduced to a thin layer due to large vacuoles (28). HyPer oxidation as a function of cytoplasmic H_2O_2 accumulation can be monitored by the ratio of fluorescence emission at 530 nm (R) after excitation at 475 nm and 438 nm. In control conditions, R was 0.25 ± 0.1, indicating that HyPer was strongly reduced. Addition of exogenous H_2O_2 (50 μM) on Col-0 epidermal peels induced an increase in R relative to its initial value (R_0), with similar amplitude and kinetics between the three different areas of preferential HyPer expression, with a peak R/R_0 value from 1.12 ± 0.02 to 1.15 ± 0.04 (Fig. S1*C*). Thus, the subcellular heterogeneity of HyPer localization in guard cells does not interfere with intracellular H_2O_2 monitoring. Exposure of guard cells to various external H_2O_2 concentrations also showed that HyPer can detect time- and dose-dependent changes in H_2O_2 concentration with a maximal R/R_0 (2.5 ± 0.1) at 2 s after addition of 200 μM H_2O_2, where most of HyPer is oxidized, and a subsequent decrease in signal in the following minute, likely due to cytoplasmic HyPer reduction (Fig. S2). A much fainter and slower transient signal was observed in response to 50 μM H_2O_2.

ABA- and flg22-Induced Guard Cell Accumulation of H_2O_2 Depends on *At*PIP2;1. We exposed the leaf epidermal peels of Col-0 and two allelic *pip2;1* mutants (*pip2;1*-1, *pip2;1*-2) to 50 μM ABA by using 0.1% ethanol as a mock (control) treatment. The changes in R/R_0 seen under the latter conditions were subtracted to the R/R_0 changes induced by ABA (Fig. S3), yielding a stimulus-specific HyPer fluorescence signal [$\Delta(R/R_0)$]. In Col-0 plants, ABA induced a transient decrease in signal, by 7 ± 0.3% after 5 min, followed by a steady increase up to 10% after 25–30 min (Fig. 1*A*, Fig. S4 *A-D*, and Movie S1). No significant difference in $\Delta(R/R_0)$ was observed between wild-type and the two *pip2;1* genotypes at 5 min after the ABA treatment [*pip2;1*-1: $\Delta(R/R_0) = -10.7 \pm 0.3\%$; *pip2;1*-2: $\Delta(R/R_0) = -4.7 \pm 0.2\%$]. However, *pip2;1* stomata did not show any subsequent increase in $\Delta(R/R_0)$ but rather a steady decrease, down to −16% and −12% for *pip2;1-1* and *pip2;1-2*, respectively (Fig. 1*A*, Fig. S4 *A* and E–G and Movie S2). To determine the contribution to $\Delta(R/R_0)$ of apoplastic H_2O_2, we pretreated Col-0 epidermal peels by catalase (200 U) (Fig. S5). This treatment abolished the intracellular H_2O_2 accumulation observed when ABA was applied, with $\Delta(R/R_0)$ decreasing by 17 ± 3% after 30 min while it increased by 10 ± 1% when ABA was applied in the absence of catalase (Fig. S5*A*). The overall data indicate that *At*PIP2;1 is necessary for ABA-dependent accumulation of H_2O_2 in guard cells, this accumulation being contributed by apoplastic H_2O_2.

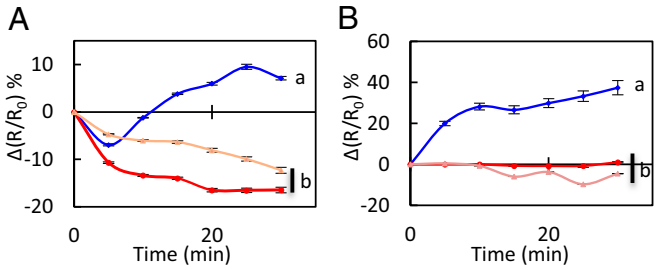

Fig. 1. Kinetic variations of HyPer fluorescence induced by ABA (*A*) or flg22 (*B*) in guard cells. Col-0 (purple diamonds), *pip2;1-1* (red squares) and *pip2;1-2* (tan triangles) epidermal peels were exposed to light during 3 h before treatment ($t = 0$) with 50 μM ABA (*A*), 1 μM flg22 (*B*) or control buffers [0.1% ethanol (*A*) or water (*B*)]. The R/R_0 measured in control guard cells was subtracted from R/R_0 in guard cells exposed to ABA or flg22, yielding $\Delta(R/R_0)$. Error bars represent SEs. Data from three independent plant cultures, each with 30 guard cells by genotype. The letters indicate statistically different values (ANOVA, Newman–Keuls: $P < 0.05$).

To possibly extend these results and test for a general role of *At*PIP2;1 in guard cell H_2O_2 transport, we investigated flg22, which also acts on stomatal movement through ROS signaling (18). Flg22 (1 μM) induced in Col-0 guard cells a marked increase in $\Delta(R/R_0)$ by 37% after 30 min (Fig. 1*B*, Fig. S4 *H–K*, and Movie S3). In contrast, *pip2;1-1* and *pip2;1-2* guard cells did not show any significant increase in $\Delta(R/R_0)$, with maximal variations of 1% and −4%, respectively (Fig. 1*B*, Fig. S4 *H* and L–N and Movie S4). In addition, the increase in $\Delta(R/R_0)$ induced in Col-0 by a 30-min treatment with flg22 (32 ± 5% in these experiments) could be partially counteracted by using exogenous catalase (9 ± 5%) (Fig. S5*B*). The overall data conform to the idea that both ABA and flg22 induce a production of H_2O_2 in Col-0 guard cell apoplasm, which, in turn, accumulates in the cytoplasm. To test the specificity of this guard cell response, we also investigated the putative role of *At*PIP2;1 in H_2O_2 transport induced by flg22 in mesophyll cell protoplasts (Fig. S6). In agreement with the low expression of *At*PIP2;1 in this cell type, we were not able to see any significant difference in the rate of H_2O_2 transport between Col-0 and *pip2;1-2* plants. As HyPer fluorescence is sensitive to pH changes, we used 2′,7′-bis-(2-carboxyethyl)-5-(and-6)-carboxyfluorescein (BCECF), a commonly used pH-sensitive fluorescent probe, to determine whether Col-0 and *pip2;1* guard cells may not exhibit specific pH changes in response to 50 μM ABA or 1 μM flg22, or their respective controls ethanol and H_2O (Fig. S7). In all conditions, the Col-0 and *pip2;1* genotypes showed similar increases in BCECF fluorescence, i.e., similar alkalinization of the cytoplasm, indicating that differences in HyPer fluorescence between Col-0 and *pip2;1* guard cells in response to ABA and flg22 reflect true differences in cytoplasmic H_2O_2 accumulation. The contribution of *At*PIP2;1 to the latter process support the role of AQP in facilitating the diffusion of H_2O_2 across the guard cell plasma membrane.

Role of *At*PIP2;1 in flg22-Induced Stomatal Closure. We next investigated whether the defect in flg22-induced H_2O_2 accumulation seen in *pip2;1* plants could be associated with a defect in stomatal closure in response to flg22, as observed for ABA (11). Stomata of Col-0 and *pip2;1* plants and of a *PIP2;1* complemented mutant line (*pip2;1-1 PIP2;1)* showed a similar opening response to a light pretreatment (Fig. 2*A*). However, stomata of *pip2;1-1* and *pip2;1-2* plants did not close in response to 1 μM flg22, whereas stomata from Col-0 and *pip2;1-1 PIP2;1* reduced their aperture by almost 40% after 2 h. Thus, *At*PIP2;1 is required for flg22-induced stomatal closure.

We previously showed that ABA activates *At*PIP2;1-mediated guard cell water transport (11). To determine if a similar mechanism

PLANT BIOLOGY

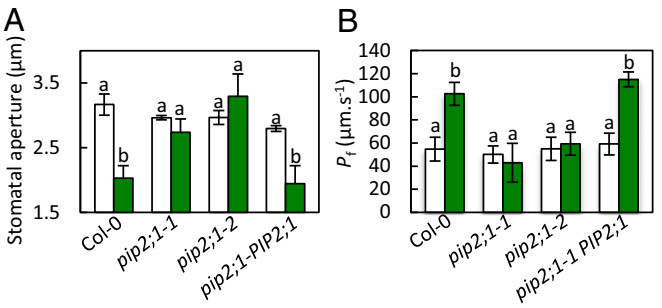

Fig. 2. Stomatal movement and water transport responses of Col-0, *pip2;1-1*, *pip2;1-2*, *pip2;1-PIP2;1* to flg22. (*A*) Epidermal peels from the indicated genotypes were placed in a bathing solution for 3 h under light and further incubated in the absence (white bars) or in the presence of 1 µM flg22 (green bars). Stomatal aperture was measured after 2 h. Data from three independent plant cultures, each with 60 stomata per genotype. Error bars represent SEs. The letters indicate statistically different values (ANOVA, Newman–Keuls: $P < 0.05$). (*B*) Guard cell protoplasts were isolated from the indicated genotypes and incubated under light in the absence (white bars) or presence (green bars) of 1 µM flg22. Their P_f was measured as described in *Materials and Methods*. Data from three independent experiments, with a total of n = 12–17 protoplasts per condition. Same conventions as in *A*.

operates in response to flg22, we investigated the effect of flg22 on the P_f of guard cell protoplasts isolated from Col-0, *pip2;1-1*, *pip2;1-2*, and *pip2;1-PIP2;1* plants. In the absence of flg22, all protoplast types had similar P_f in the range of 50–60 µm·s^{-1} (Col-0: $P_f = 55 \pm 10$ µm·s^{-1}). Treatment with 1 µM flg22 increased twofold the P_f of Col-0 (103 ± 10 µm·s^{-1}) and *pip2;1-1 PIP2 ;1* guard cell protoplasts (Fig. 2*B*). In contrast, the P_f of *pip2;1-1* and *pip2;1-2* guard cell protoplasts was totally unresponsive to flg22. Thus, flg22, similar to ABA, increases the water transport activity of *At*PIP2;1 in guard cells.

Contribution of *At*PIP2;1 To Guard Cell Transport of H_2O_2 in Response to flg22 and ABA. In view of the activation by ABA and flg22 of *At*PIP2;1-dependent P_f, we investigated whether *At*PIP2;1-mediated H_2O_2 transport is also ABA- and flg22-dependent. Epidermal peels were first pretreated by flg22 (1 µM), ABA (10 µM), or their respective control solution (water or 0.02% ethanol, respectively). Kinetic variations of guard cell R/R_0 were then monitored, following sudden exposure to exogenous H_2O_2 (100 µM) (Fig. 3). When epidermal peels of Col-0, *pip2;1-1*, or *pip2;1-2* plants were submitted to control pretreatments, exogenous H_2O_2 induced a similar slow and progressive increase in R/R_0, up to a maximum of 1.4, with a slight decay after 30–40 s (Fig. 3 *A*–*F*). Col-0 epidermal peels pretreated by flg22 (Fig. 3*A*) showed a faster HyPer oxidation response to H_2O_2, with a peak R/R_0 value of 1.69 ± 0.05 reached at 24 s after H_2O_2 addition. In contrast, *pip2;1-1* and *pip2;1-2* guard cells pretreated with flg22 (Fig. 3 *B* and *C*) showed an HyPer oxidation response similar to that after a control pretreatment, with a maximum R/R_0 value reached for both genotypes after 42 s of exposure to exogenous H_2O_2.

ABA also enhanced the HyPer oxidation response of Col-0 guard cells to exogenous H_2O_2, with R/R_0 reaching a maximum of 1.67 ± 0.02 after 37 s (Fig. 3*D*). By comparison, R/R_0 in ethanol-pretreated peels showed a maximum of 1.16 ± 0.03 at 45 s following addition of H_2O_2. At variance with Col-0, *pip2;1-1* and *pip2;1-2* guard cells (Fig. 3 *E* and *F*) showed similar and low-amplitude HyPer oxidation response to exogenous H_2O_2, whether pretreated or not with ABA. The data show that pretreatments with flg22 or ABA promote the accumulation of exogenously supplied H_2O_2 in Col-0 guard cells. The lack of such effects in *pip2;1* plants suggests that ABA and flg22 activate *At*PIP2;1 to increase the guard cell membrane permeability to H_2O_2.

Protein Kinases Involved in PAMP and ABA Signaling Are Crucial for *At*PIP2;1 Function During flg22-Induced Stomatal Closure. To determine the PAMP signaling components involved in activation of *At*PIP2;1 by flg22, we investigated the effect of the peptide on the P_f of guard cell protoplasts isolated from Col-0, *fls2 efr*, *snrk2.6*, and *bak1-5* plants (Fig. 4), considering that *bak1-5* is a semidominant allele of *BAK1* with a specific phenotype related to PAMP responsiveness (29). In the absence of flg22, all protoplast types had similar P_f in the range of 53–65 µm·s^{-1} (Col-0: $P_f = 60 \pm 10$ µm·s^{-1}). While treatment with 1 µM flg22 increased twofold the P_f of Col-0 (113 ± 13 µm·s^{-1}), the P_f of *fls2 efr*, *bak1-5*, and *snrk2.6* guard cell protoplasts was totally unresponsive to flg22. The P_f of guard cell protoplasts was also insensitive to 10 µM ABA in *snrk2.6*, whereas it was enhanced by twofold in Col-0 (132 ± 8 µm·s^{-1}; ref. 11). The overall data indicate that, in guard cells, flg22 increases *At*PIP2;1 water transport activity by acting through its receptor (FLS2) and interacting coreceptor (BAK1). Interestingly, OST1 is involved in activation of *At*PIP2;1-mediated water transport by both ABA and flg22.

Role of *At*PIP2;1 Ser121 in flg22-Induced Guard Cell Functions. Phosphorylation of *At*PIP2;1 at Ser121 is mandatory for stimulation of both guard cell protoplast P_f and stomatal closure by ABA (11). In vitro phosphorylation (11) and genetic analyses (Fig. 4) suggest that this effect is mediated by OST1. Because the effects of flg22 on guard cell water transport also depend on OST1, we investigated the possible role of Ser121 phosphorylation in this mechanism. We used a *pip2;1-2* line expressing phosphorylation-deficient (S121A) or phosphomimetic (S121D) forms of *At*PIP2;1 (11). S121A protoplasts displayed moderate P_f values that were insensitive to a flg22 treatment (Control, $P_f = 57 \pm 2$ µm·s^{-1}; flg22, $P_f = 57 \pm 3$ µm·s^{-1}) and similar to those in *pip2;1-2* plants or Col-0 plants in control conditions (Fig. S8). S121D plants displayed significantly higher P_f values which, however, were also insensitive to flg22 (Control, $P_f = 82 \pm 3$ µm·s^{-1}; flg22, $P_f = 86 \pm 2$ µm·s^{-1}).

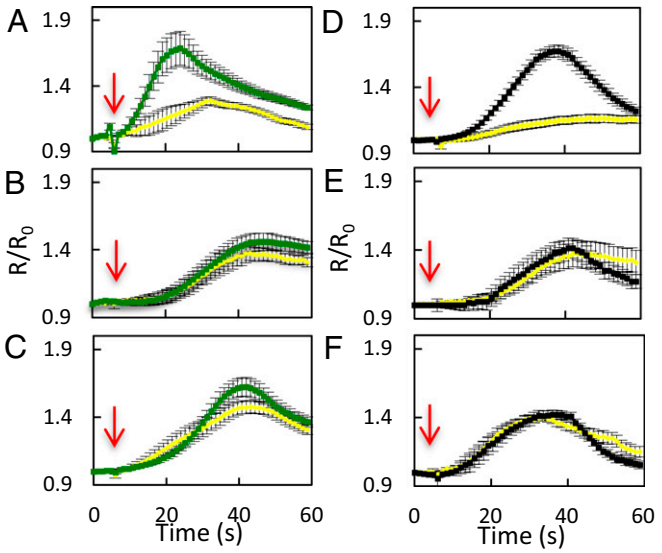

Fig. 3. Influx of exogenously supplied H_2O_2in guard cells of Col-0, *pip2;1-1*, and *pip2;1-2* plants. Epidermal peels from Col-0 (*A* and *D*), *pip2;1-1* (*B* and *E*) or *pip2;1-2* (*C* and *F*) plants were placed under light for 3 h and subsequently treated for 6 min by flg22 (1 µM) (green) or water (yellow) (*A*–*C*) or by ABA (10 µM) (black) or ethanol (0.02%) (yellow) (*D*–*F*) before application of exogenous H_2O_2. Kinetic changes in HyPer fluorescence (R/R_0) were recorded before and after the application of 100 µM H_2O_2 (red arrow at $t = 5$ s). Error bars represent the SEs from measurements cumulating three independent plant cultures, with a total between 30 and 40 guard cells per genotype.

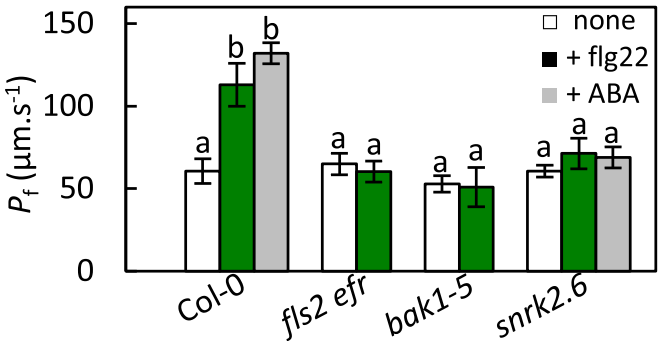

Fig. 4. Water transport responses of Col-0, *fls2 efr*, *bak1-5*, and *snrk2;6* to light, flg22, and ABA. Guard cell protoplasts were isolated from the indicated genotypes and incubated under light in the absence (white bars) or presence of 1 µM flg22 (green bars) or 10 µM ABA (gray bars). Their P_f was measured as described in *Materials and Methods*. Data from three independent experiments, with a total of $n = 7–10$ protoplasts per condition. Error bars represent SEs. The letters indicate statistically different values (ANOVA, Newman–Keuls: $P < 0.05$).

These data indicate that phosphorylation of *At*PIP2;1 on Ser121 is necessary for stimulation of guard cell P_f by flg22.

Because of the crucial role of BAK1 in flg22-dependent activation of *At*PIP2;1, we investigated the ability of recombinant BAK1 to modify *At*PIP2;1 peptides in an in vitro phosphorylation assay with ^{32}P-labeled ATP (Fig. S9*A*). In this assay, BAK1 efficiently labeled the generic protein kinase substrate MBP. A C-terminal *At*PIP2;1 peptide containing two well described phosphorylation sites at Ser280 and Ser283 was poorly phosphorylated by BAK1 (Fig. S9*A*), whereas a 29-residue peptide covering the entire *At*PIP2;1 loop *B* was markedly labeled. While this peptide includes Ser121 and two other Ser/Thr residues, no radiolabeling was observed when Ser121 was substituted by an Ala residue (S121A). The dose dependency of peptide labeling by BAK1 indicated an apparent K_m of the protein kinase for the loop *B* peptide of 18.2 ± 5 µM (Fig. S9*B*). These data indicate that, albeit with a lower affinity than OST1, BAK1 can phosphorylate *At*PIP2;1, preferentially at Ser121.

We next wondered if the *At*PIP2;1-dependent H_2O_2 transport activity observed in response to flg22 (Fig. 3*A* and Fig. S10*A*) also depends on Ser121 phosphorylation. We expressed HyPer in the S121A and S121D lines and monitored guard cell HyPer oxidation kinetics. S121A guard cells showed variations of R/R_0 in response to exogenous H_2O_2 that were similar and of low amplitude, whether the epidermis was pretreated or not with flg22 (Fig. S10*B*). This profile is reminiscent of that seen in *pip2;1-2* plants (Fig. 3 *B* and *C*). Flg22 pretreatment did not alter the HyPer oxidation signal to exogenous H_2O_2 in S121D guard cells either (Fig. S10*C*). However, these plants showed, both in the absence or presence of a flg22 pretreatment, high R/R_0 peak values of 1.82 ± 0.01 and 1.68 ± 0.02, respectively, at 26 s after exposure to exogenous H_2O_2 (Fig. S10 *B* and *C*). The data strongly suggest that Ser121 phosphorylation mediates the stimulating effects of flg22 on the guard cell permeability to H_2O_2.

We next investigated the significance of this *At*PIP2;1 regulation mechanism in integrated responses of stomata to flg22. The peptide induced a marked H_2O_2 accumulation in both Col-0 and S121D stomata (Fig. 5) with, after 30 min, a maximal increase in $\Delta(R/R_0)$ of 37% and 46%, respectively. In contrast, S121A guard cells, similar to *pip2;1-2*, lacked this response and showed a $\Delta(R/R_0)$ decreasing by 6% after 30 min. With regard to flg22-induced stomatal closure, expression of the Ser121A form of *At*PIP2;1 was not able to complement the defect of *pip2;1-2* plants whereas expression of the S121D form restored a stomatal closure response similar to Col-0 plants (Fig. S11). In addition, application of catalase on Col-0 or S121D epidermal peels fully abolished the stomatal closure observed in the presence of flg22, thereby mimicking the lack of stomatal response of *pip2;1* plants to flg22 (Fig. S12). Altogether, these data pinpoint the requirement of *At*PIP2;1 Ser121 phosphorylation for flg22-induced accumulation of H_2O_2 in guard cells and subsequent stomatal closure.

Discussion

Signaling Function of *At*PIP2;1 in Guard Cells. We previously established an essential role of *At*PIP2;1 in ABA-induced stomatal closure (11). In this initial study, we screened abiotic stimuli acting on stomatal movements and found no obvious involvement of *At*PIP2;1 in guard cell response to CO_2, light or darkness. In line with *At*PIP2;1 contribution to ABA-induced stomatal closure, the P_f of guard cell protoplasts was enhanced by ABA through activation of *At*PIP2;1. Assays using H_2DCFDA, a generic ROS probe, also revealed a defect of *pip2;1* plants in ABA-dependent ROS signaling, indicating that the role of *At*PIP2;1 in guard cells may go beyond its canonical water channel function. Independent growth tests and transport assays using H_2DCFDA have established, indeed, that *At*PIP2;1 can facilitate ROS diffusion in yeast (24, 30). In addition, a role in plant defense was recently attributed to the *At*PIP1;4 homolog, based on its ability to transport H_2O_2 in the mesophyll (26). Thus, we assumed that AQPs and *At*PIP2;1 in particular may play a general role in H_2O_2-dependent signaling. Here, we used the guard cell system and investigated stimuli which, besides ABA, involve H_2O_2 signaling. The role of *At*PIP2;1 in flg22-induced stomatal closure was therefore uncovered.

Another key point was to use the genetically encoded H_2O_2 sensor HyPer for kinetic monitoring of intracellular H_2O_2 in various genetic backgrounds. This approach was instrumental to show that both ABA and flg22 trigger within a few minutes an accumulation of H_2O_2 in the guard cell cytoplasm. We also showed that this accumulation was not due to possible confounding effects of the AQP on cytosolic pH but originates from H_2O_2 produced in the apoplasm and requires *At*PIP2;1.

Another important analogy between ABA and flg22 is that they both enhance within minutes the water permeability P_f of the guard cell plasma membrane. We therefore assumed that the associated activation of *At*PIP2;1 may also play a role in H_2O_2 transport. Although our assay cannot be considered as a genuine measurement of H_2O_2 membrane permeability, the finding that flg22 and ABA pretreatments favor the influx of exogenous H_2O_2 in an *At*PIP2;1-dependent manner provides strong evidence that *At*PIP2;1 transports H_2O_2 through the guard cell plasma membrane,

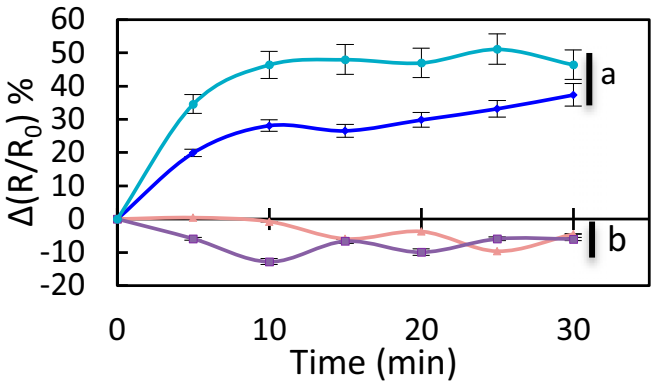

Fig. 5. Kinetic variations of HyPer fluorescence induced by flg22 in guard cells of Col-0 (blue diamonds), *pip2;1-2* (tan triangles), S121A (purple squares), and S121D (sky blue circles) plants. Same procedures and conventions as in Fig. 1*B*. Data from three independent plant cultures, each with at least 30 guard cells by genotype.

thereby contributing to ABA and flg22 signaling during stomatal closure. *At*PIP1;4 also plays a signaling role during PAMP-triggered immunity (26), but whether this aquaporin is also activated during this process remains unknown. As *At*PIP2;1 is the most abundant PIP2 in guard cells, we speculate that transport by PIP1s of water and/or H_2O_2 at the plasma membrane may require heteromerization with PIP2s, and preferentially *At*PIP2;1, thereby explaining the strong stomatal phenotype of the single pip2;1 mutants. Altogether, these findings are reminiscent of results obtained in animal cells. A pioneering work using HyPer unraveled the role of AQP3 in H_2O_2 transport and epidermal growth factor (EGF) signaling (31). This function was recently extended to NF-κB signaling in keratinocytes (32) or in response to environmental stresses in colonic epithelia (33). Similarly, AQP8 facilitates cellular accumulation of H_2O_2 after VEGF stimulation, thereby enhancing PI3K activity and phosphorylation of MAPKs, two essential processes for leukemia cell proliferation (34).

Combined with our previous work (11), the present study indicates that the contribution of *At*PIP2;1 to guard cell responses to ABA and flg22 involves both a signaling and a hydraulic function. Interestingly, *pip2;1* plants showed impaired stomatal movements in response to ABA (11) and flg22 (this study) instead of a reduced rate of closure, as could be expected from a simple decrease in cell water permeability. This suggests that the signaling function of *At*PIP2;1 may somewhat dominate in these contexts. However, a hydraulic and a signaling role are not exclusive. As H_2O_2 and water share the same permeation path within single AQP monomers (35), mechanisms acting on AQP function, such as phosphorylation, similarly enhance water and H_2O_2 transport. Thus, *At*PIP2;1 may facilitate H_2O_2 influx into the guard cell during the early phase of ABA or flg22 perception and, subsequently, facilitate water efflux from the guard cell, thereby contributing to stomatal closure. The ROS signaling function of *At*PIP2;1 may also be relevant in other tissues or organs where *At*PIP2;1 operates such as bundle sheaths (36) or roots (37). In the latter case, *At*PIP2;1 was shown to facilitate the emergence of lateral roots, a process known to involve ROS (38). These ideas are not exclusive of other cell signaling functions of *At*PIP2;1, such as extracellular CO_2 transport and signaling in guard cells (25). In this case, however, parallel transport of CO_2 through the lipid membrane or other *At*PIP isoforms may have prevented the detection of a defective stomatal response to CO_2 in *pip2;1* plants (25).

Signaling Specificity and Cross-Talks in Guard Cells. Signaling pathways inducing stomatal closure in response to ABA and pathogens are increasingly well documented (3, 14). We recently proposed that phosphorylation of *At*PIP2;1 at Ser121, by OST1 and possibly other protein kinases, is critical for increasing guard cell water transport in response to ABA (11). The present study extends these observations showing the essential role of *At*PIP2;1 Ser121 phosphorylation in flg22-induced guard cell transport of water and H_2O_2. Accordingly, *At*PIP2;1 Ser121 phosphorylation was required for stomatal closure in response to both ABA (11) and flg22 (Fig. S11). Interestingly, the corresponding residue (Ser126) of a barley PIP homolog seems to be crucial for H_2O_2 transport in yeast (39, 40).

In the case of pathogen infection, PAMPs and DAMPs are perceived as general signals for stomatal closure, thereby limiting plant infection. Early signaling elements, which include H_2O_2, nitric oxide, or calcium lead to activation of RbohD NADPH oxidase and SLAC1 anion channel, are shared among the PAMP, DAMP, and ABA response pathways. In agreement with earlier studies proposing a role for OST1 in guard cell responses to flg22, including activation of SLAC1 (12, 20), the protein kinase was also required for flg22-dependent activation of *At*PIP2;1. Knowing that OST1 is activated by BAK1 during guard cell response to ABA (41), it may be regulated in a similar way in response to flg22. This model fits with the idea that BAK1 acts as a relay between the flg22 receptor FLS2 and downstream components. In these respects, it was somewhat surprising that recombinant BAK1 can also phosphorylate *At*PIP2;1 on Ser121. Because BAK1 showed a fivefold higher K_m than OST1 in this assay and flg22-dependent activation of P_f was cancelled in both *bak1-5* and *snrk2.6*, we rather favor the idea that *At*PIP2;1 is activated through a nonredundant pathway whereby BAK1 activates OST1 which, in turn, phosphorylates *At*PIP2;1 at Ser121.

Although our study points to commonalities between ABA and flg22 signaling, with H_2O_2 acting as a central hub, distinct patterns of ROS can be observed in response to specific stimuli (42). In molecular terms, flg22 activates ABA-independent signaling components, such as oxylipins and salicylic acid, together with specific protein kinases (19). These include BIK1 and CPK5, which were recently shown to phosphorylate RbohD (18, 43), or CPK4, CPK6, and CPK11, which function as positive regulators of the PAMP-induced ROS burst (44). Along with these lines, our study suggests that ABA and flg22 induced distinct kinetics and intensities of H_2O_2 accumulation in the guard cell cytoplasm. In particular, ABA induces an *At*PIP2;1-independent decrease in HyPer signal after 5 min, which was not observed upon flg22 treatment. This ABA-specific response, whether of extracellular or intracellular origin, may reflect distinct modes of RbohD activation by ABA and flg22, or alternatively, distinct effects of the two stimuli on cytosolic pH. Finally, our work highlights the importance of intracellular H_2O_2 signaling in guard cells. While key proteins such as glutathione peroxidase 3 (*At*GPX3) (45) or ABI2 protein phosphatase (46) are known to be regulated through ROS-dependent oxidation, other cellular targets of H_2O_2 may play an important role during stomatal closure and not restricted to guard cell responses to flg22 and ABA. Ethylene and methyl jasmonate (MeJA) also induce H_2O_2 production (14, 47) to promote stomatal closure, thereby protecting the plant from dehydration and/or pathogen attacks. While *At*PIP2;1 is the only detected PIP2 expressed in guard cells (48), several PIP1s are also expressed, which may transport H_2O_2 (24, 30). Thus, a potential role of other AQPs in ethylene and MeJA-induced stomatal closure remains to be investigated.

In conclusion, this work has improved our general knowledge of plant cell signaling, by showing that an AQP can have a signaling function, here in the context of ABA- and flg22-induced stomatal closure. In addition, the activating role of specific protein kinases was uncovered. The use of HyPer, a specific H_2O_2 probe, opens perspectives to address more generally the role of other AQPs in H_2O_2 transport, a process that is attracting a growing interest in physiology. For instance, H_2O_2 was proposed to mediate long-distance signaling in plant tissues (49). Together with NADPH oxidases, AQPs may be crucial for signal propagation, in analogy with the role of ion channels in electrical signaling.

Materials and Methods

Plant Materials. All experiments were performed in *A. thaliana* Col-0 or its derivatives. The aquaporin genotypes (*pip2;1-1*, *pip2;1-2*, *pip2;1-PIP2;1*, S121A, S121D) and signaling mutants (*fls2c efr-1*, *bak1-5, snrk2.6*) were as described in ref. 11 and refs. 29, 50, and 51, respectively. Aquaporin lines expressing a cytoplasmic form of HyPer under the control of a double enhanced cauliflower mosaic virus 35S promoter (28) were obtained by crossing as described in *SI Materials and Methods*.

Physiological Responses. Stomatal aperture was measured on epidermal peels excised from the abaxial side of leaves of 3- to 4-wk-old plants as described (11). Guard cell protoplasts were prepared from approximately 50 leaves (11), and their osmotic P_f was measured by using an osmotic swelling assay according to a described procedure (52). Additional information on plant growth conditions or measurements of stomatal aperture or P_f can be found in *SI Materials and Methods*.

Guard Cell Fluorescence Imaging. Epidermal fragments isolated from leaves of 3-wk-old *Arabidopsis* plants were attached to microscope coverslips by using a silicone adhesive (Telesis 5; Paris Berlin) and incubated in a bathing

solution (30 mM KCl, 10 mM Mes/Tris, pH 6.0) for 3 h under constant light (~300 $\mu E \cdot m^{-2} \cdot s^{-1}$). Guard cells expressing HyPer were analyzed by using an inverted fluorescence microscope (Zeiss Axioplan) with a 40× immersion oil objective. Excitation light was produced by a monochromator (Lumencor) at 475/428 nm and 438/424 nm. The two excitation wavelengths were delivered as alternating pulses (100 ms), and the emitted light deflected by dichroic mirrors (HC BS 506) was collected through emission filters (BP 536/540). Images were acquired by using a CCD camera (Cooled SNAP HQ, Photometrics). Synchronization of the monochromator and CCD camera was performed through a control unit run by a Fluorescence Ratio Imaging software (MetaFluor). Image analysis was performed with an ImageJ software. For time course experiments, fluorescence intensity in guard cells was determined over regions of interest, at 530 nm after excitation at 438 nm or 475 nm (E_i438 and E_i475). Background fluorescence signals were measured in regions outside the cell, using similar excitation and emission wavelengths (E_b438 and E_b475), and subtracted from corresponding fluorescence values measured in guard cells. A fluorescence ratio R was calculated as $R = (E_i475 - E_b475)/(E_i438 - E_b438)$. Changes in fluorescence over time were expressed with respect to the initial ratio R_0 as R/R_0. Imaging of the ratiometric pH sensitive probe BCECF was performed by a similar approach as described in *SI Materials and Methods*.

In Vitro Phosphorylation. Phosphorylation assays using recombinant BAK1 and *At*PIP2;1 peptides were as described in *SI Materials and Methods*.

ACKNOWLEDGMENTS. We thank the Plant Growth Facility personnel of the Biochemistry and Plant Molecular Physiology department. O.R. and A.G. were both supported by doctoral fellowships from the French Ministry of Higher Education and Research while G.R. was supported by an Erasmus Mundus EUROEAST grant from the European Commission. This publication reflects the views only of the author, and the Commission cannot be held responsible for any use which may be made of the information contained therein.

1. Hetherington AM, Woodward FI (2003) The role of stomata in sensing and driving environmental change. *Nature* 424:901–908.
2. Roelfsema MR, Hedrich R (2005) In the light of stomatal opening: New insights into 'the Watergate'. *New Phytol* 167:665–691.
3. Kim TH, Böhmer M, Hu H, Nishimura N, Schroeder JI (2010) Guard cell signal transduction network: Advances in understanding abscisic acid, CO_2, and Ca^{2+} signaling. *Annu Rev Plant Biol* 61:561–591.
4. Park SY, et al. (2009) Abscisic acid inhibits type 2C protein phosphatases via the PYR/PYL family of START proteins. *Science* 324:1068–1071.
5. Joshi-Saha A, Valon C, Leung J (2011) A brand new START: Abscisic acid perception and transduction in the guard cell. *Sci Signal* 4:re4.
6. Kwak JM, et al. (2003) NADPH oxidase AtrbohD and AtrbohF genes function in ROS-dependent ABA signaling in Arabidopsis. *EMBO J* 22:2623–2633.
7. Sirichandra C, et al. (2009) Phosphorylation of the Arabidopsis AtrbohF NADPH oxidase by OST1 protein kinase. *FEBS Lett* 583:2982–2986.
8. Brandt B, et al. (2012) Reconstitution of abscisic acid activation of SLAC1 anion channel by CPK6 and OST1 kinases and branched ABI1 PP2C phosphatase action. *Proc Natl Acad Sci USA* 109:10593–10598.
9. Geiger D, et al. (2009) Activity of guard cell anion channel SLAC1 is controlled by drought-stress signaling kinase-phosphatase pair. *Proc Natl Acad Sci USA* 106:21425–21430.
10. Lee SC, Lan W, Buchanan BB, Luan S (2009) A protein kinase-phosphatase pair interacts with an ion channel to regulate ABA signaling in plant guard cells. *Proc Natl Acad Sci USA* 106:21419–21424.
11. Grondin A, et al. (2015) Aquaporins contribute to ABA-triggered stomatal closure through OST1-mediated phosphorylation. *Plant Cell* 27:1945–1954.
12. Melotto M, Underwood W, Koczan J, Nomura K, He SY (2006) Plant stomata function in innate immunity against bacterial invasion. *Cell* 126:969–980.
13. Lozano-Durán R, Bourdais G, He SY, Robatzek S (2014) The bacterial effector HopM1 suppresses PAMP-triggered oxidative burst and stomatal immunity. *New Phytol* 202:259–269.
14. McLachlan DH, Kopischke M, Robatzek S (2014) Gate control: Guard cell regulation by microbial stress. *New Phytol* 203:1049–1063.
15. Dou D, Zhou JM (2012) Phytopathogen effectors subverting host immunity: Different foes, similar battleground. *Cell Host Microbe* 12:484–495.
16. Mersmann S, Bourdais G, Rietz S, Robatzek S (2010) Ethylene signaling regulates accumulation of the FLS2 receptor and is required for the oxidative burst contributing to plant immunity. *Plant Physiol* 154:391–400.
17. Khokon AR, et al. (2011) Involvement of extracellular oxidative burst in salicylic acid-induced stomatal closure in Arabidopsis. *Plant Cell Environ* 34:434–443.
18. Kadota Y, et al. (2014) Direct regulation of the NADPH oxidase RBOHD by the PRR-associated kinase BIK1 during plant immunity. *Mol Cell* 54:43–55.
19. Montillet JL, Hirt H (2013) New checkpoints in stomatal defense. *Trends Plant Sci* 18:295–297.
20. Guzel Deger A, et al. (2015) Guard cell SLAC1-type anion channels mediate flagellin-induced stomatal closure. *New Phytol* 208:162–173.
21. Maurel C, et al. (2015) Aquaporins in plants. *Physiol Rev* 95:1321–1358.
22. Uehlein N, Lovisolo C, Siefritz F, Kaldenhoff R (2003) The tobacco aquaporin NtAQP1 is a membrane CO_2 pore with physiological functions. *Nature* 425:734–737.
23. Dynowski M, Schaaf G, Loque D, Moran O, Ludewig U (2008) Plant plasma membrane water channels conduct the signalling molecule H_2O_2. *Biochem J* 414:53–61.
24. Bienert GP, Chaumont F (2014) Aquaporin-facilitated transmembrane diffusion of hydrogen peroxide. *Biochim Biophys Acta* 1840:1596–1604.
25. Wang C, et al. (2016) Reconstitution of CO_2 regulation of SLAC1 anion channel and function of CO_2-permeable PIP2;1 aquaporin as carbonic anhydrase 4 interactor. *Plant Cell* 28:568–582.
26. Tian S, et al. (2016) Plant aquaporin AtPIP1;4 links apoplastic H2O2 induction to disease immunity pathways. *Plant Physiol* 171:1635–1650.
27. Belousov VV, et al. (2006) Genetically encoded fluorescent indicator for intracellular hydrogen peroxide. *Nat Methods* 3:281–286.
28. Costa A, et al. (2010) H_2O_2 in plant peroxisomes: An in vivo analysis uncovers a $Ca^{(2+)}$-dependent scavenging system. *Plant J* 62:760–772.
29. Schwessinger B, et al. (2011) Phosphorylation-dependent differential regulation of plant growth, cell death, and innate immunity by the regulatory receptor-like kinase BAK1. *PLoS Genet* 7:e1002046.
30. Bienert GP, et al. (2007) Specific aquaporins facilitate the diffusion of hydrogen peroxide across membranes. *J Biol Chem* 282:1183–1192.
31. Miller EW, Dickinson BC, Chang CJ (2010) Aquaporin-3 mediates hydrogen peroxide uptake to regulate downstream intracellular signaling. *Proc Natl Acad Sci USA* 107:15681–15686.
32. Hara-Chikuma M, et al. (2015) Aquaporin-3-mediated hydrogen peroxide transport is required for NF-κB signalling in keratinocytes and development of psoriasis. *Nat Commun* 6:7454.
33. Thiagarajah JR, Chang J, Goettel JA, Verkman AS, Lencer WI (2017) Aquaporin-3 mediates hydrogen peroxide-dependent responses to environmental stress in colonic epithelia. *Proc Natl Acad Sci USA* 114:568–573.
34. Vieceli Dalla Sega F, et al. (2014) Specific aquaporins facilitate Nox-produced hydrogen peroxide transport through plasma membrane in leukaemia cells. *Biochim Biophys Acta* 1843:806–814.
35. Cordeiro RM (2015) Molecular dynamics simulations of the transport of reactive oxygen species by mammalian and plant aquaporins. *Biochim Biophys Acta* 1850:1786–1794.
36. Prado K, et al. (2013) Regulation of Arabidopsis leaf hydraulics involves light-dependent phosphorylation of aquaporins in veins. *Plant Cell* 25:1029–1039.
37. Péret B, et al. (2012) Auxin regulates aquaporin function to facilitate lateral root emergence. *Nat Cell Biol* 14:991–998.
38. Manzano C, et al. (2014) The emerging role of reactive oxygen species signaling during lateral root development. *Plant Physiol* 165:1105–1119.
39. Rhee J, Horie T, Sasano S, Nakahara Y, Katsuhara M (2017) Identification of an H2 O2 permeable PIP aquaporin in barley and a serine residue promoting H2 O2 transport. *Physiol Plant* 159:120–128.
40. Bienert GP, Heinen RB, Berny MC, Chaumont F (2014) Maize plasma membrane aquaporin ZmPIP2;5, but not ZmPIP1;2, facilitates transmembrane diffusion of hydrogen peroxide. *Biochim Biophys Acta* 1838:216–222.
41. Shang Y, Dai C, Lee MM, Kwak JM, Nam KH (2016) BRI1-associated receptor kinase 1 regulates guard cell ABA signaling mediated by open stomata 1 in Arabidopsis. *Mol Plant* 9:447–460.
42. Song Y, Miao Y, Song CP (2014) Behind the scenes: The roles of reactive oxygen species in guard cells. *New Phytol* 201:1121–1140.
43. Boudsocq M, et al. (2010) Differential innate immune signalling via $Ca^{(2+)}$ sensor protein kinases. *Nature* 464:418–422.
44. Dubiella U, et al. (2013) Calcium-dependent protein kinase/NADPH oxidase activation circuit is required for rapid defense signal propagation. *Proc Natl Acad Sci USA* 110:8744–8749.
45. Miao Y, et al. (2006) An Arabidopsis glutathione peroxidase functions as both a redox transducer and a scavenger in abscisic acid and drought stress responses. *Plant Cell* 18:2749–2766.
46. Meinhard M, Rodriguez PL, Grill E (2002) The sensitivity of ABI2 to hydrogen peroxide links the abscisic acid-response regulator to redox signalling. *Planta* 214:775–782.
47. Daszkowska-Golec A, Szarejko I (2013) Open or close the gate - stomata action under the control of phytohormones in drought stress conditions. *Front Plant Sci* 4:138.
48. Leonhardt N, et al. (2004) Microarray expression analyses of *Arabidopsis* guard cells and isolation of a recessive abscisic acid hypersensitive protein phosphatase 2C mutant. *Plant Cell* 16:596–615.
49. Gilroy S, et al. (2014) A tidal wave of signals: Calcium and ROS at the forefront of rapid systemic signaling. *Trends Plant Sci* 19:623–630.
50. Nekrasov V, et al. (2009) Control of the pattern-recognition receptor EFR by an ER protein complex in plant immunity. *EMBO J* 28:3428–3438.
51. Yoshida R, et al. (2002) ABA-activated SnRK2 protein kinase is required for dehydration stress signaling in Arabidopsis. *Plant Cell Physiol* 43:1473–1483.
52. Ramahaleo T, Morillon R, Alexandre J, Lassalles J-P (1999) Osmotic water permeability of isolated protoplasts. Modifications during development. *Plant Physiol* 119:885–896.

Supporting Information

Rodrigues et al. 10.1073/pnas.1704754114

SI Materials and Methods

Plant Materials and Growth Conditions. All experiments were performed in *A. thaliana* Col-0 or derived transgenic lines. The *pip2;1-1*, *pip2;1-2, pip2;1-PIP2;1*, S121A, and S121D lines were described in ref. 11. These lines were crossed with Col-0 plants expressing a cytoplasmic form of HyPer under the control of a double enhanced cauliflower mosaic virus 35S promoter (28). Homozygous genetic backgrounds containing the HyPer transgene were selected by a series of PCR with the following primers: 5′-GACTCGAGATGGCAAAGGATGTGGCAGCCGTTC-3′ and 5′-GAGATACCGGCGGTGCAGTAG-3′ for Col-0, 5′-TGCAGCAAAACCCACACTTTTACTTC-3′ and 5′-GAGCGTCGGTCCCCACATTCTATAC-3′ for *pip2;1-1*, 5′-GCTTGTTGAACCGACACTTTTAACATAAG-3′ and 5′- GAGATACCGGCGGTGCAGTAG-3′ for *pip2;1-2*, 5′-GACTCGAGATGGCAAAGGATGTGGCAGCCGTTC-3′ and 5′-CCCTAGGTAAAGCCACTTTACGTGCC-3′ for S121A, 5′-GACTCGAGATGGCAAAGGATGTGGCAGCCGTTC-3′ and 5′-CCCYAGGTAAATCCACTTTACGTGCC-3′ for S121D. The presence of the HyPer transgene was also determined by PCR using 5′-CCCGAATCCAAAATGGAGATGGCAAGCCAGGGC-3′ and 5′-CCCGAATTCTTAAACCGCCTGTTTTAAAAC-3′ primers and its expression was characterized by imaging at 530 nm after excitation at 438 nm or 475 nm. For subsequent protoplast isolation, stomatal assays, or HyPer imaging, plants were grown in soil (NeuhausHuminSubstrat N2; Klasman-Deilmann) in controlled growth chambers with a relative humidity of 70% under 8-h light (250 $\mu E \cdot m^{-2} \cdot s^{-1}$) at 22 °C/16-h dark at 21 °C cycles.

Measurements of Stomatal Aperture. Stomatal aperture was measured on epidermal peels excised from the abaxial side of leaves of 3- to 4-wk-old plants as described (11). In all experiments, epidermal peels of the indicated genotypes were first incubated for 30 min in darkness at ambient air in a bathing solution (30 mM KCl, 1 mM $CaCl_2$, 10 mM Mes/Tris, pH 6.0), before exposure to the indicated treatments. Average stomatal aperture was then measured every hour in a minimum of 60 stomata on two epidermis fragments from two independent plants. Experiments were repeated three times for each of three independent plant cultures. In studies with flg22, dark adapted epidermal peels were first exposed to white light (300 $\mu E \cdot m^{-2} \cdot s^{-1}$) for 180 min, to induce maximal stomatal opening. One micromolar flg22 was then added to the bathing solution, and stomatal aperture was monitored during the next 120 min.

Osmotic Water Permeability of Guard Cell Protoplasts. Guard cell protoplasts were prepared as described in ref. 11 from approximately 50 leaves. Isolated protoplasts were resuspended in 4 mL of solution A (0.57 M sorbitol, 0.5 mM ascorbic acid, 0.5 mM $MgCl_2$, 0.5 mM $CaCl_2$, 5 mM Mes, pH 5.5) and kept under darkness before exposure to light (300 $\mu E \cdot m^{-2} \cdot s^{-1}$) and treatment with 1 μM flg22 or 10 μM ABA for 45 min. Guard cell protoplasts were identified according to their size (7–15 μm) and their low chloroplast content. Swelling measurements were performed at 20 °C by transferring individual protoplasts into a hypotonic solution B (solution A but with 0.42 M sorbitol) under microscope using a described procedure (52). The osmotic ratio between solutions A and B allows a theoretical protoplast swelling of 36%. All protoplasts showing nonlinear initial swelling kinetics or a volume increase <16% or >56% were discarded from the analyses.

In Vitro Phosphorylation. Phosphorylation assays on specific *At*PIP2;1 peptides were performed essentially as described (11). The BAK1 cytoplasmic kinase domain (starting at Lys299 to stop codon) was purified from BL21-Rosetta *E. coli* cells harboring a pMALc2-BAK1 construct and purified on MBP-Trap affinity columns. All synthetic peptides used in this study were purified to >80% by HPLC (Proteogenix). They correspond to the following *At*PIP2;1 domains: the loop *B* either wild-type (loopB: MACTAGISGGHINPAVTFGLFLARKV*S*LPRAKKK) or with a S121A mutation (loopB_S121A: MACTAGISGGHINPAVTFGLFLARKV*A*LPRAKKK) or the C-terminal tail (Cter: MASKSLGSFRSAANVKKK). The myelin basic protein (Sigma) was used as a generic kinase substrate. In all experiments, *At*PIP2;1 peptides (1–100 μM) or MBP (20 ng/μL) were incubated at 25 °C in 250 μL of a reaction mixture containing 250 ng of purified BAK1, 100 μM [γ^{32}P]ATP (0.1 $\mu Ci \cdot nmol^{-1}$), 25 mM β-glycerophosphate, 20 mM $MgCl_2$, 1 mM DTT, 50 mM Hepes, pH 7.4. At selected time points, 40-μL aliquots of the reaction mixture were spotted on a P81 phosphocellulose paper and rapidly dried. P81 paper was washed for 3 × 10 min in 0.85% phosphoric acid, once in acetone and dried. Radioactivity was measured on a Packard TRI-CARB phosphor imager.

BCECF Imaging. Epidermal fragments isolated from leaves of 3-wk-old *Arabidopsis* plants were attached to microscope coverslips by using a silicone adhesive (Telesis 5, Paris Berlin) and incubated in a bathing solution (30 mM KCl, 10 mM Mes/Tris, pH 6.0) for 3 h under constant light (~300 $\mu E \cdot m^{-2} \cdot s^{-1}$). One hundred nanomolar BCECF-acetoxymethyl (AM) ester (ThermoFisher Scientific) was added to the bathing solution from a 1 mM stock solution in DMSO. BCECF-AM is a nonpolar, unreactive molecule which diffuses intracellularly where its AM ester group is cleaved by endogenous esterases to yield BCECF. After 15 min in the presence of BCECF-AM, epidermal peels were thoroughly washed four consecutive times with fresh bathing solution, to eliminate all remaining extracellular dye. To monitor H^+ content of guard cells, a randomly chosen epidermal peal area containing 10–20 stained stomata was observed under constant light (250 $\mu E \cdot m^{-2} \cdot s^{-1}$). BCECF fluorescence was analyzed by using an inverted fluorescence microscope (Zeiss Axioplan) with a 40× immersion oil objective. Excitation light was produced by a monochromator (Lumencor) at 475/428 nm and 438/424 nm. The two excitation wavelengths were delivered as alternating pulses (100 ms), and the emitted light deflected by dichroic mirrors (HC BS 506) was collected through emission filters (BP 536/540). Images were acquired by using a CCD camera (Cooled SNAP HQ, Photometrics). Synchronization of the monochromator and CCD camera was performed through a control unit run by a Fluorescence Ratio Imaging software (MetaFluor). Image analysis was performed with an ImageJ software. For time course experiments, fluorescence intensity in guard cells was determined over regions of interest, at 530 nm after excitation at 438 nm or 475 nm (E_i438 and E_i475). Background fluorescence signals were measured in regions outside the cell, using similar excitation and emission wavelengths (E_b438 and E_b475), and subtracted from corresponding fluorescence values measured in guard cells. A fluorescence ratio (FR) was calculated as $FR = (E_i475 - E_b475)/(E_i438 - E_b438)$.

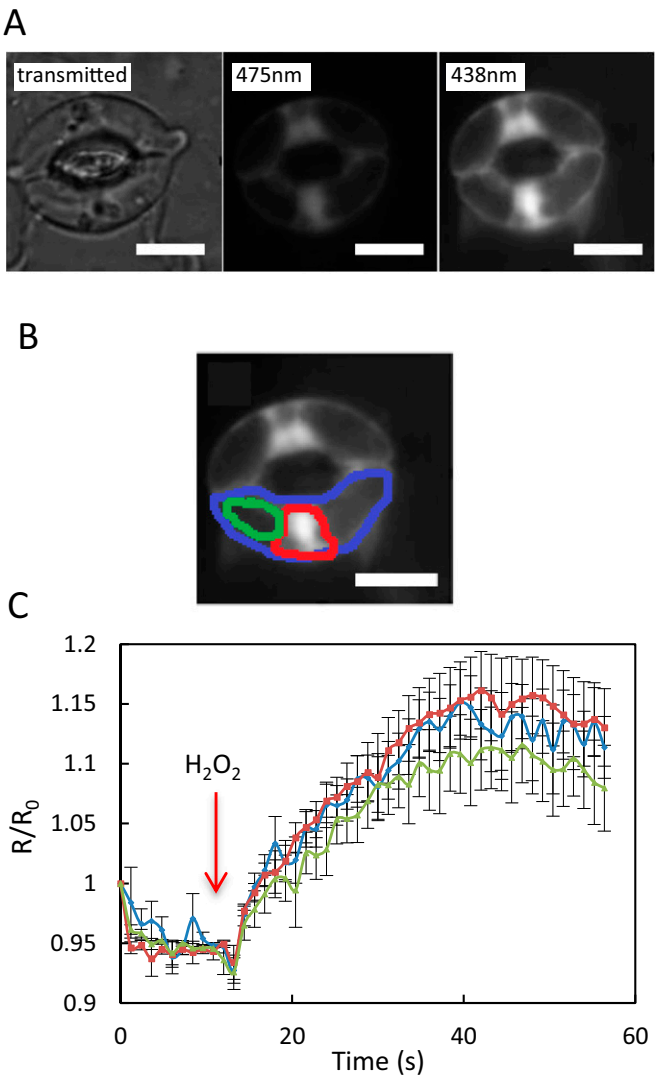

Fig. S1. Expression and oxidation of HyPer in distinct *A. thaliana* guard cell zones in response to exogenous H_2O_2. (*A*) Leaf epidermal peels were observed by microscopy under visible or fluorescent light. Excitation of the oxidized and reduced states of HyPer was performed at 475 nm and 438 nm, respectively, and emission was detected at 530 nm in both cases. (*B*) Areas selected for kinetic analysis of relative changes in fluorescence ratio (R/R_0): whole cell (blue diamonds), nucleus and its periphery (red squares), and a region occupied by large vacuoles (green triangles). (*C*) Time course of R/R_0 variations for the three zones described in *A*. Fifty micromolar H_2O_2 was added to the epidermal peel at $t = 10$ s (arrow). Error bars represent SEs from average measurements on 8–12 guard cells. (Scale bars: 5 μm.)

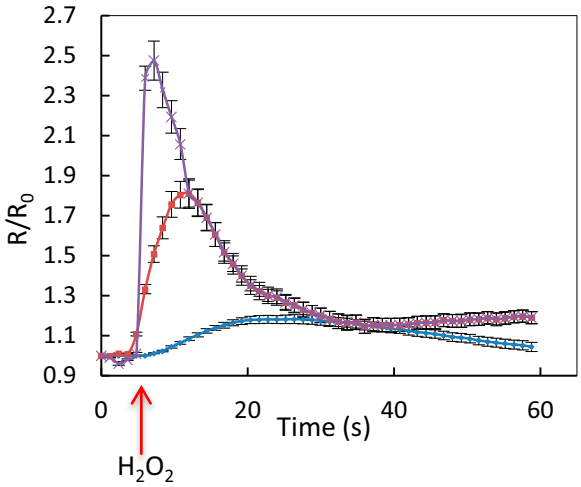

Fig. S2. Kinetics of HyPer oxidation in Col-0 guard cells in response to exogenous H_2O_2. Epidermal peels were exposed from $t = 5$ s to three exogenous H_2O_2 concentrations: 50 μM (blue diamonds), 100 μM (red squares), and 200 μM (purple cross), and R/R_0 was measured over time. The error bars represent SEs from average measurements on 8–12 guard cells.

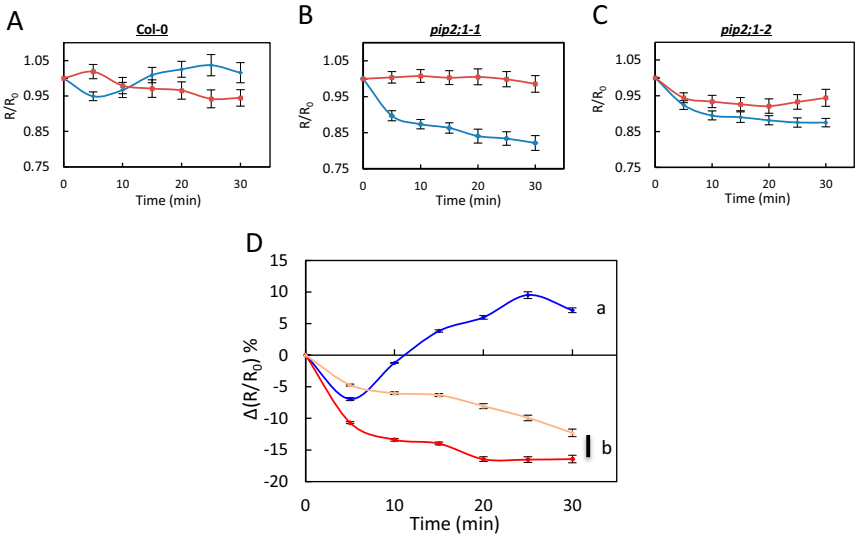

Fig. S3. Kinetic variations of HyPer signal induced by exogenous ABA in Col-0 and *pip2;1* guard cells. (*A*–*C*) Epidermal peels from Col-0 (*A*), *pip2;1-1* (*B*), and *pip2;1-2* (*C*) plants were exposed to light during 3 h before exposure at $t = 0$ to ABA (50 μM) (blue diamonds) or a control treatment (0.1% ethanol) (red squares). R/R_0 was measured in guard cells at the indicated time. (*D*) The graph shows a plot, at each time point and for each genotype (Col-0: blue diamonds; *pip2;1-1*: red circles; *pip2;1-2*: tan triangles) of the difference in R/R_0 (Fig. 1*A*) between ABA-treated and control guard cells [$\Delta(R/R_0)$]. Error bars represent SEs.

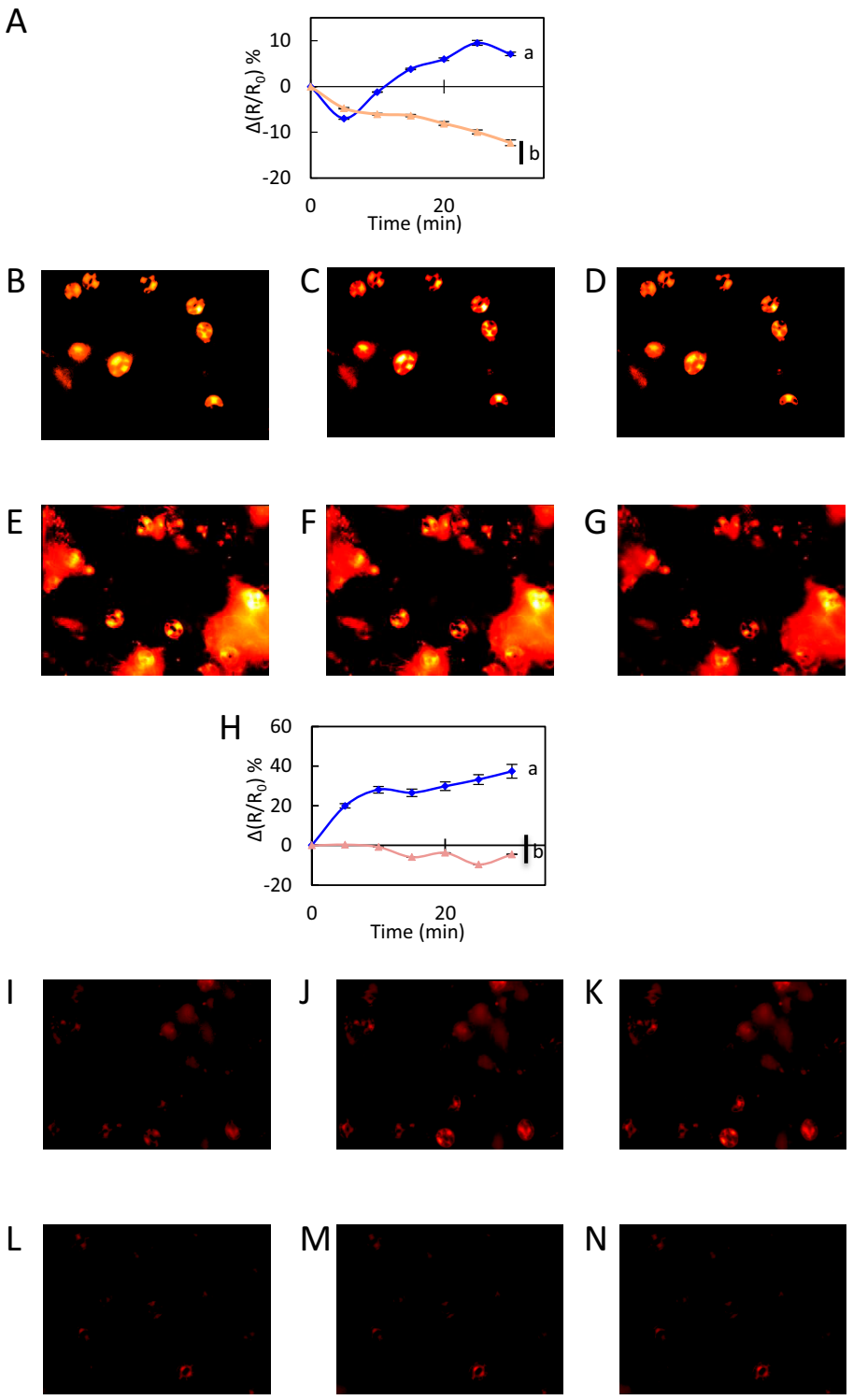

Fig. S4. Kinetic variations of HyPer fluorescence induced by flg22 in guard cells. Col-0 (blue diamonds) and *pip2;1-2* (tan triangles) epidermal peels were exposed to light during 3 h before treatment ($t = 0$) with 50 μM ABA (*A*–*G*) or 1 μM flg22 (*H*–*N*) as described in Fig. 1. Representative images of changes of HyPer fluorescence ratio (R) are shown at $t = 0$ (*B*, *E*, *I*, and *L*), $t = 20$ min (*C*, *F*, *J*, and *M*), and $t = 30$ min (*D*, G, *K*, and *N*). As cumulative data shown in Fig. 1 and in *A* and *H* is the average of three independent experiments with more than 30 guard cells analyzed, the images shown here do not reflect perfectly the average ratio changes measured in this study. Movies of the whole kinetics are also available (Movies S1–S4).

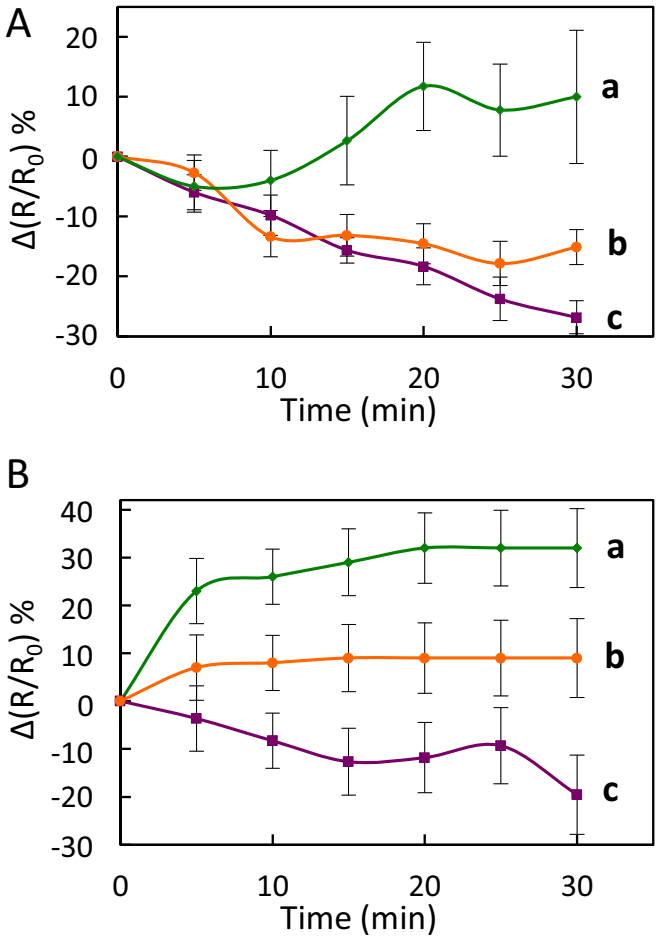

Fig. S5. Effects of catalase on the changes in HyPer fluorescence [$\Delta(R/R_0)$] induced by ABA (*A*) or flg22 (*B*) in Col-0 guard cells. Epidermal peels were exposed to light for 3 h before exposure (at $t = 0$) to 50 μM ABA (*A*) or 1 μM flg22 (*B*), in the presence (orange circles) or in the absence (green diamonds) of 200 U catalase. A control treatment at $t = 0$ with catalase alone (purple squares) was also performed. Time-dependent variations in $\Delta(R/R_0)$ were calculated by reference to untreated epidermis as exemplified in Fig. S3. Error bars represent SEs. Data are from three independent plant cultures, with at least 30 guard cells per genotype and experiment. The letters indicate statistically different values (ANOVA, Newman–Keuls: $P < 0.05$).

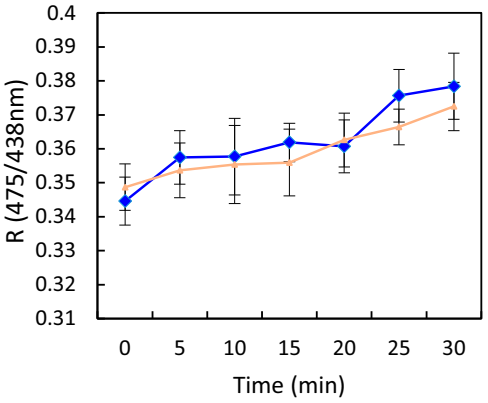

Fig. S6. Kinetic variations of HyPer signal induced by exogenous flg22 in mesophyll cell protoplasts of Col-0 and *pip2;1-2*. Protoplasts from Col-0 (blue diamonds) and *pip2;1-2* (tan triangles) plants were exposed to light during 2 h before exposure at $t = 0$ to flg22 (1 μM). Ratiometric fluorescence (R) of HyPer with excitations at 475 and 438 nm was measured at the indicated time. Error bars represent SEs. Data are from at least 50 mesophyll protoplasts per genotype and experiment.

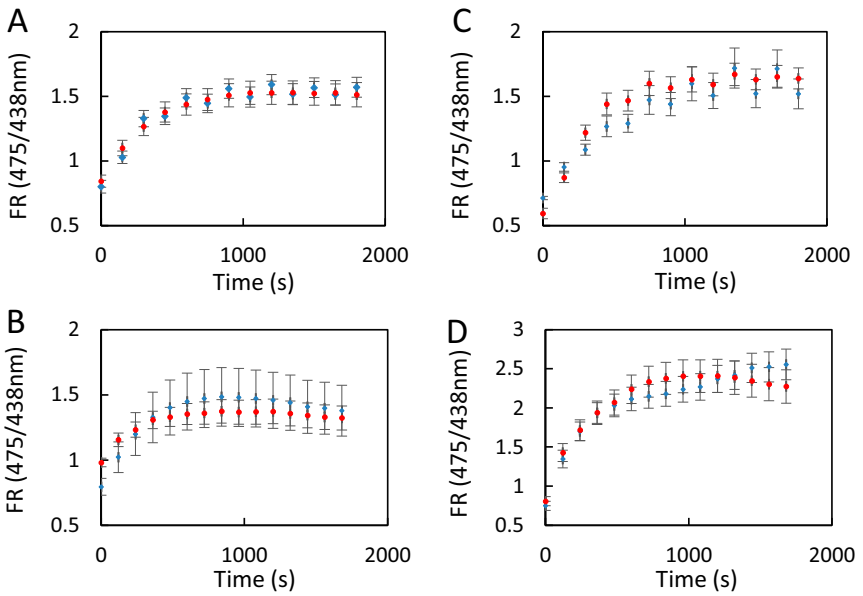

Fig. S7. Kinetic variations of BCECF signal induced by exogenous ABA or flg22 and their respective control treatments in Col-0 and *pip2;1-1* guard cells. Epidermal peels from Col-0 (blue diamonds) or *pip2;1-1* (red circles) plants were exposed to light during 3 h before exposure at $t = 0$ to ABA (50 μM) (*A*) or its control treatment (0.1% ethanol) (*B*) or to flg22 (1 μM) (*C*) or its control treatment (H_2O) (*D*). An FR at 530 nm was calculated as FR = ($E_i475–E_b475$)/($E_i438–E_b438$) after excitation of the unprotonated and protonated states of BCECF at 475 nm and 438 nm, respectively, and measured in guard cells at the indicated time. Error bars represent SEs. Data from three independent plant cultures, each with >150 guard cells by genotype.

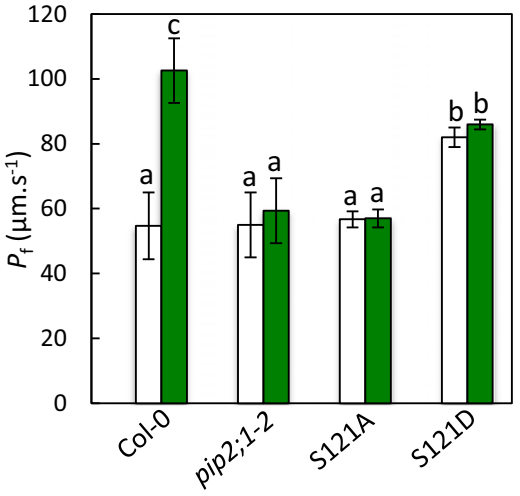

Fig. S8. Effect of flg22 on P_f of guard cell protoplasts from Col-0, *pip2;1-2*, S121A, and S121D plants. Guard cell protoplasts were isolated from the indicated genotypes and incubated under light in the absence (white bars) or in the presence (green bars) of 1 μM flg22. Their P_f was measured as described in *Materials and Methods*. Data from three independent plant cultures, with a total of $n = 12–17$ protoplasts per condition. The letters indicate statistically different values (ANOVA, Newman–Keuls: $P < 0.05$).

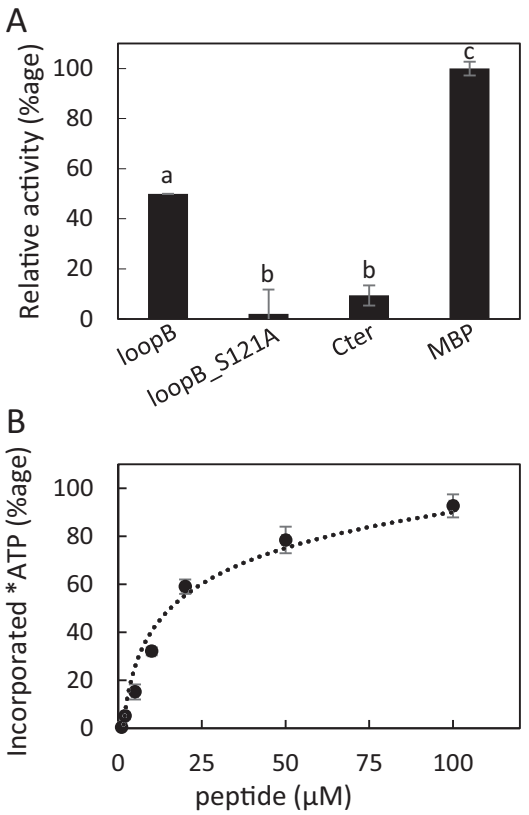

Fig. S9. In vitro phosphorylation of *At*PIP2;1 peptides by BAK1. (*A*) Phosphorylation by purified BAK1 of native or mutated peptides from the loop B and C-terminal region of *At*PIP2;1. Incorporated ATP (±SE) from $n = 4$ independent experiments was normalized to the signal observed with the reference myelin basic protein (MBP). (*B*) The loop B *At*PIP2;1 peptide was incubated at the indicated concentrations, in the presence of labeled ATP and purified BAK1. The mean incorporated ATP (±SE) was determined from four independent experiments, each with 2–3 technical replicates. Calculated affinity (K_m) is = 18.2 ± 5 μM.

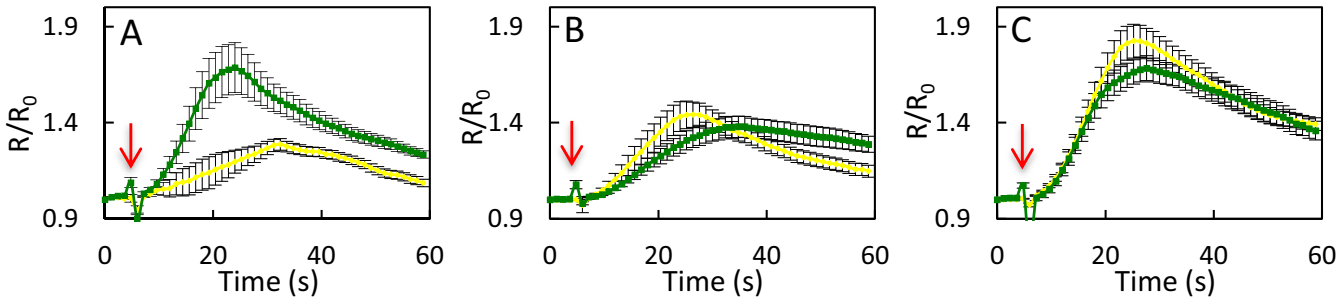

Fig. S10. Influx of exogenously supplied H_2O_2 in guard cells of Col-0, S121A, and S121D plants. Epidermal peels from Col-0 (*A*), S121A (*B*), or S121D (*C*) plants were placed under light during 3 h and subsequently treated by flg22 (1 μM) (green squares) or water (yellow squares) for 6 min. Kinetic changes in HyPer fluorescence (R/R_0) were recorded before and after the application of 100 μM H_2O_2 (red arrow at $t = 5$ s). Error bars represent the SEs from measurements cumulated from three independent plant cultures, with a total between 30 and 40 guard cells per genotype.

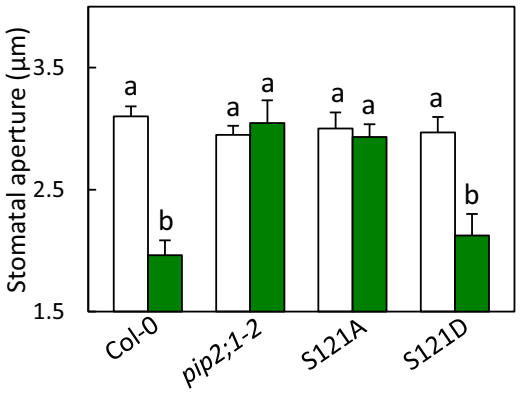

Fig. S11. Stomatal movement response of Col-0, *pip2;1-2*, S121A, and S121D plants to flg22. Epidermal peels from the indicated genotypes were incubated in a bathing solution under light for 3 h, before application of 1 μM flg22 (green bars) or a mock treatment (white bars). Stomatal aperture was measured after 2 h. Data from three independent plant cultures, with a total of at least 60 stomata per condition. Error bars represent SEs. Letters indicate statistically different values (ANOVA, Newman–Keuls: $P < 0.05$).

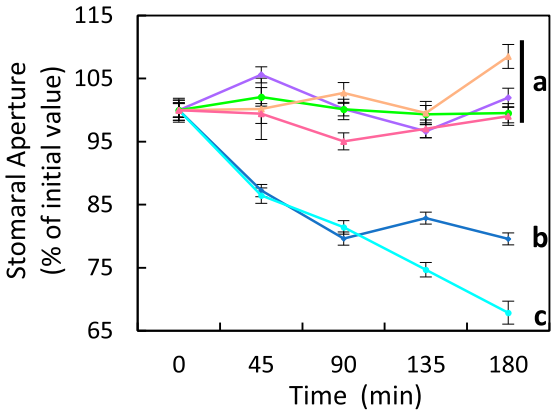

Fig. S12. Effects of catalase on the stomatal response of Col-0, *pip2;1-2*, and S121D plants to flg22. Epidermal peels from the indicated genotypes were incubated in a bathing solution under light for 3 h, before application of 1 μM flg22 in the presence (Col-0: purple diamonds; *pip2;1-2*: pink triangles; S121D: green circles) or absence (Col-0: blue diamonds; *pip2;1-2*: tan triangles; S121D: sky blue circles) of 200 U of catalase. Stomatal aperture was measured every 30 min for 3 h. Data from three independent plant cultures, with a total of at least 80 stomata per condition. Error bars represent SEs. Letters indicate statistically different values (ANOVA, Newman–Keuls: $P < 0.05$).

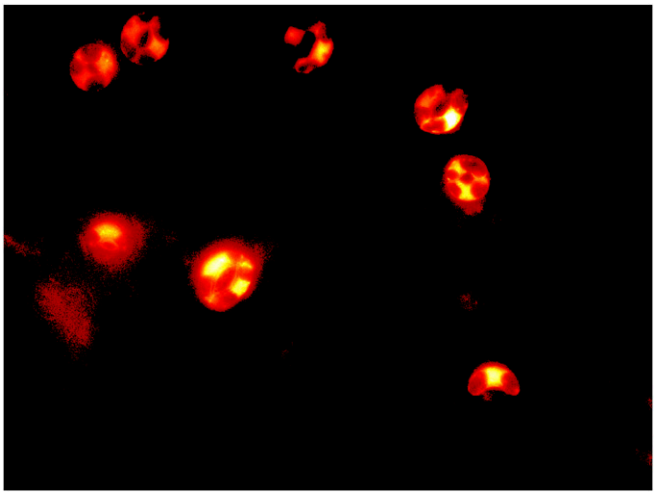

Movie S1. Fluorescence time-lapse movie of changes of HyPer fluorescence ratio of Col-0 epidermal peels exposed to 50 μM ABA for 30 min. Ratios are obtained every 5 min. See also Fig. S4 *B–D*.

Movie S1

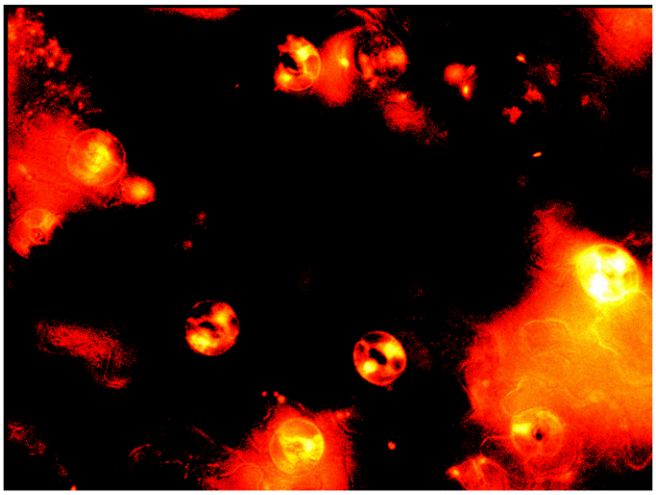

Movie S2. Fluorescence time-lapse movie of changes of HyPer fluorescence ratio of *pip2;1-2* epidermal peels exposed to 50 μM ABA for 30 min. Ratios are obtained every 5 min. See also Fig. S4 *E–G*.

Movie S2

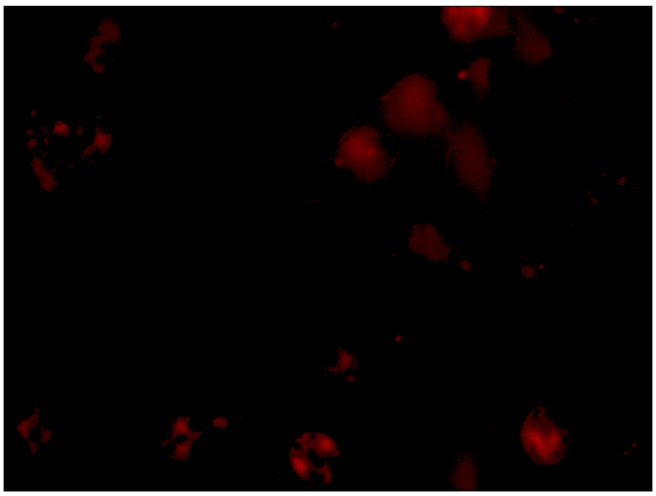

Movie S3. Fluorescence time-lapse movie of changes of HyPer fluorescence ratio of Col-0 epidermal peels exposed to 1 μM ABA for 30 min. Ratios are obtained every 5 min. See also Fig. S4 *I–K*.

Movie S3

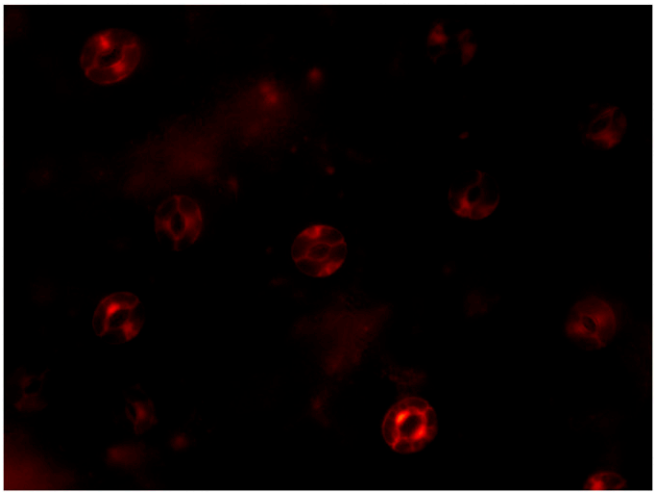

Movie S4. Fluorescence time-lapse movie of changes of HyPer fluorescence ratio of *pip2;1-2* epidermal peels exposed to 1 μM ABA for 30 min. Ratios are obtained every 5 min. See also Fig. S4 *L*–N.

Movie S4